Purdue University
Purdue e-Pubs

International Compressor Engineering Conference | School of Mechanical Engineering

2014

Development of Rotary Compressor for High-efficiency CO2 Heat-pump Hot-Water Supply System

Takeshi Chinen
Toshiba Carrier Corporation, Japan, takeshi.chinen@toshiba.co.jp

Hisataka Kato
Toshiba Carrier Corporation, Japan, hisataka.kato@toshiba.co.jp

Masaya Ichihara
Toshiba Carrier Corporation, Japan, masaya.ichihara@glb.toshiba.co.jp

Hiroyuki Mizuno
Toshiba Carrier Corporation, Japan, hiroyuki.mizuno@glb.toshiba.co.jp

Follow this and additional works at: https://docs.lib.purdue.edu/icec

Chinen, Takeshi; Kato, Hisataka; Ichihara, Masaya; and Mizuno, Hiroyuki, "Development of Rotary Compressor for High-efficiency CO2 Heat-pump Hot-Water Supply System" (2014). *International Compressor Engineering Conference.* Paper 2339.
https://docs.lib.purdue.edu/icec/2339

This document has been made available through Purdue e-Pubs, a service of the Purdue University Libraries. Please contact epubs@purdue.edu for additional information.
Complete proceedings may be acquired in print and on CD-ROM directly from the Ray W. Herrick Laboratories at https://engineering.purdue.edu/Herrick/Events/orderlit.html

Development of Rotary Compressor for High-efficiency CO2 Heat-pump Hot-water Supply System

Takeshi CHINEN*, Hisataka KATO, Masaya ICHIHARA, Hiroyuki MIZUNO

Compressor Design Department, Toshiba Carrier Corporation,
336, Tadewara, Fuji City, Shizuoka Prefecture, 416-8521 JAPAN
Tel: +81-545-62-5641, Fax; +81-545-55-0305
takeshi.chinen@toshiba.co.jp, hisataka.kato@toshiba.co.jp
masaya.ichihara@glb.toshiba.co.jp, hiroyuki.mizuno@glb.toshiba.co.jp

* Corresponding Author

ABSTRACT

In Japan, there has been an increase in the use of domestic heat-pump hot-water supply systems in which the refrigerant is CO2, which does not cause ozone layer depletion and has a low global-warming potential. In addition, in recent years, there has been an increase in the number of examples in which CO2 is employed as a refrigerant for showcase refrigerators, freezers etc. Therefore, in the future, it is expected that there will be an increasing demand for CO2 compressors with greater efficiency and lower noise. In the case of domestic heat-pump hot-water supply systems, in order to increase the annual performance factor (APF) of a product, it is effective to enhance the coefficient of performance (COP) in an intermediate capacity range. Here, we report the development of a high-APF rotary compressor achieved by optimizing the design specifications of a motor and a discharge pathway from a discharge chamber, for operation in the intermediate capacity range. In the optimization process, in order to cope with the high operating pressure of the CO2 water-heating cycle, we performed analysis using the finite element method (FEM) for evaluating the stiffness around the discharge port. In addition, we used an FEM model of the entire compressor in a modal analysis, and, in analyzing the radiation surfaces of the rotary compressor, we used an acoustic particle velocity probe that is capable of measuring the intensity at an intermediate portion between the accumulator and the compressor main unit, where it has been difficult to take measurements in the past. We also discuss an example in which noise reduction was confirmed when the specifications of the accumulator were changed based on the results of these analyses.

1. INTRODUCTION

Since the Fukushima nuclear power plant accident caused by the Tohoku earthquake and tsunami of March 2011, there is a greater awareness about energy saving among the general public than ever before. Agency for natural resources and energy (2013) observed that supplying hot water accounts for 28 % of household energy consumption in Japan, and thus, it is of considerable importance to enhance the energy-saving capacity of heat-pump hot-water supply systems. As with air conditioners, the annual performance factor (APF) has been introduced as an indicator of the energy efficiency for heat-pump hot-water supply systems, and the efficiency of equipment has been enhanced in accordance with the actual performance. In order to reduce power consumption over the course of a year while maintaining sufficient hot-water capacity required for the winter, it is important to enhance the coefficient of performance (COP) in the intermediate capacity range, which accounts for a large proportion of the operating time. We have developed a rotary compressor with a higher APF than an original compressor by optimizing the characteristics of the compression mechanism and motor for operation in the intermediate capacity range.

In addition, because domestic heat-pump hot-water supply systems are operated during nighttime when electricity charges are lower, low-noise operation is required. In a domestic heat-pump hot-water supply system, because the compressor is installed in a machine compartment in the outdoor unit, with a soundproofing material surrounding

the compressor, high-frequency noise is considerably reduced by the housing, and thus, the compressor noise characteristics of interest are at low frequencies, in particular, 2 kHz or less. In one of our compressors (in the following, refer as "the original compressor"), noise in the 1.25-kHz band is greater than the noise in other bands. In this study, by using an FEM-based modal analysis and a sound radiation analysis using an acoustic particle velocity probe, we found that noise in the 1.25-kHz band was radiated from the accumulator. We also confirmed that the noise level in the 1.25-kHz band was improved by changing the specifications of the accumulator.

2. FEATURES OF CO2 ROTARY COMPRESSOR

Figure 1 shows a cross section of the CO2 rotary compressor. The basic structure of this rotary compressor is the same as that of a rotary compressor used in an air conditioner. Figure 2 shows a compression mechanism of the compressor. Because a CO2 water-heating cycle has a higher operating pressure and differential pressure as compared with an air-conditioning cycle using R410A or R32, the sliding portion between the vane and the rolling-piston is subjected to a greater load. Sufficient reliability is ensured by applying Diamond-like Carbon (DLC) processing to the vane and also by using polyalkylene glycol (PAG) oil, which has superior temperature-viscosity characteristics. As for the motor, like twin rotary compressor for air conditioner with R410A refrigerant, we used a concentrated-winding motor using a rare-earth magnet, which achieves high motor efficiency. In general, when a rare-earth magnet is used, the size of the rotor can be reduced because the magnetic flux density is higher than that of a ferrite magnet; however, with a conventional motor of our compressors for air conditioner, the inertia of the rotor is low relative to the high torque fluctuations of a CO2 single rotary compressor, which makes the controllability inferior, thus having an adverse effect on the operable operation speed, the range of operating conditions, and the performance. Because of this, we have newly developed a motor in which the rotor diameter ratio (the ratio of the external rotor diameter to the internal shell diameter) is increased. Figure 3 shows the developed motor rotor. In addition, when using CO2, Koyama *et al.* (2005) showed that the performance of a heat exchanger deteriorates when the amount of oil discharge is high. We achieved a reduction in the amount of oil discharge by providing a gas pathway in the rotor and by providing an oil separating plate for separating oil contained in gas that has passed through the gas pathway.

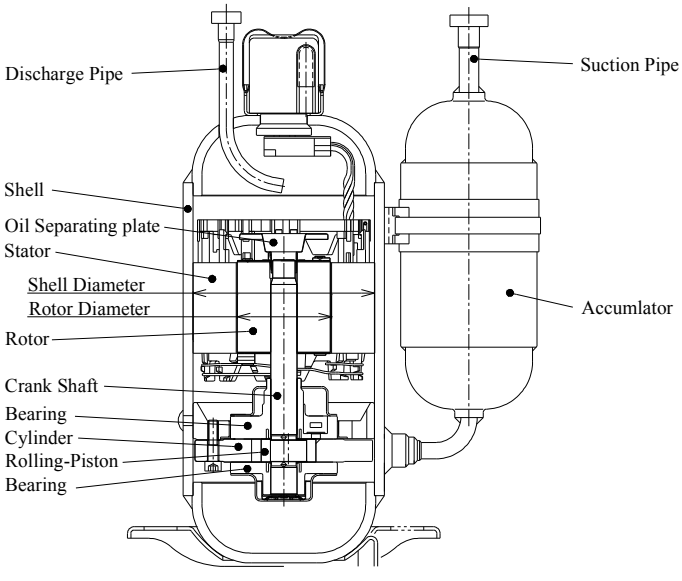

Figure 1: CO2 rotary compressor

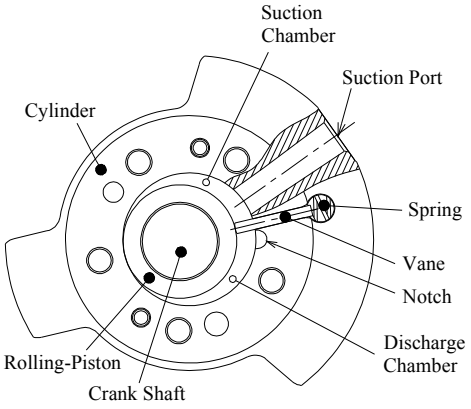

Figure 2: Compression Mechanism

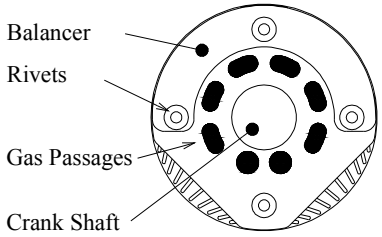

Figure 3: Motor rotor

3. IMPROVING THE APF

3.1 Improved compression mechanism

Because gas inside the discharge port and a notch in the cylinder of a rotary compressor is not discharged from the discharge chamber but is re-expanded, these two volumes are referred to as the dead volume, and re-expansion loss can be reduced by decreasing the dead volume. A value called the ideal flow velocity is obtained by dividing the amount of change in volume of the compression chamber per 1° of change in crank angle by the cross-sectional area of outlet of the compression chamber shown in Figure 4, and this value can be considered as a reference for the magnitude of over-compression loss.

$$u(\theta) = (V(\theta) - V(\theta + \alpha) / (\alpha \cdot S(\theta)) \qquad (1)$$

$u(\theta)$:Ideal Flow Velocity at Crank Angle θ
$V(\theta)$:Volume of Discharge Chamber at Crank Angle θ
$S(\theta)$:Cross-Sectional Area of outlet of Discharge Chamber at Crank angle θ
θ :Crank Angle
α :Const.

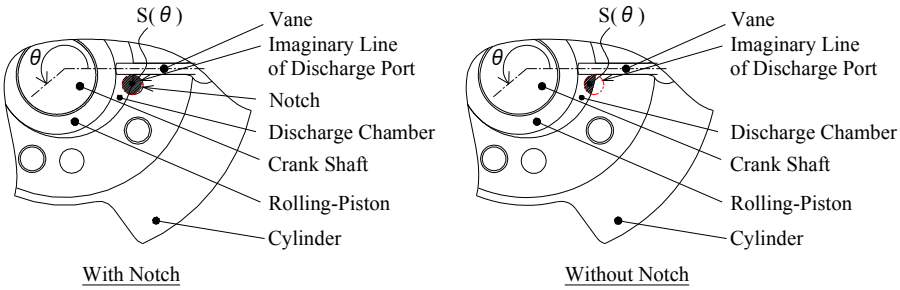

Figure 4: Cross-Sectional Area of outlet of Discharge Chamber

Generally, a notch is provided in a cylinder in order to use full of a cross-sectional area of discharge port effectively. The solid line in figure 5 shows the relationship of crank angle and ideal flow velocity ratio, where the maximum speed of gas flow at discharge port is assumed to be 100 %. In contrast, when the notch in the cylinder is eliminated without changing the port position, effective cross-sectional area of discharge port is cut by about half. The broken line in figure 5 shows the relationship of crank angle and ideal flow velocity ratio in this condition. The chain line in figure 5 shows relationship of crank angle and ideal flow velocity ratio where the notch in the cylinder is eliminated and discharge port position is shifted toward the center of the cylinder by 1mm. The flow velocity is two-times higher when the notch in the cylinder is eliminated without changing discharge port position. However, the increase in the flow velocity can be reduced to a factor of 1.4 by shifting the position of the discharge port toward the center of the cylinder by 1mm. Therefore, shifting a discharge port position toward the center of a cylinder is considered as an effective way to reduce the increase of over compression loss by eliminating the notch in cylinder. The test conditions are shown in Table 1.

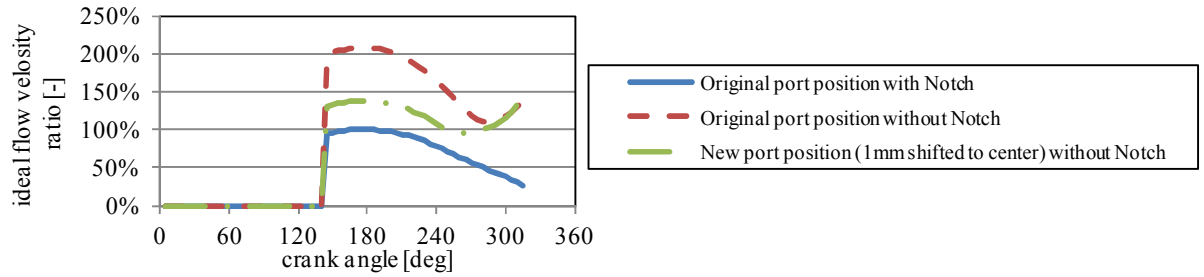

Figure 5: Relationship between crank angle and ideal flow velocity ratio

Table 1: Test conditions

Discharge Pressure [MPa]	Suction Pressure [MPa]	Temprature before an expansion valve [deg C]	Suction Temperature [deg C]
9.70	4.28	25.00	18.00

Figure 6 shows a cross section of compression mechanism. Because a large deformation around the discharge port adversely affects reliability and performance, a numerical analysis was performed on the amount of deformation during differential-pressure actuation in order to determine the thickness of the discharge port that constitutes the dead volume. Figure 7 shows an example of deformation analysis result. Table 2 shows deformation ratios, where the maximum displacement at a thin-wall portion around a port of a compressor used for air conditioner is assumed to be 100 %. The analysis results indicated that, although the thickness of the discharge port required to achieve a deformation ratio of 100 % was 3.7 mm when the flange height of the bearing was set to be 7 mm, as in the compressor for air-conditioner, it is possible to reduce this value to 2.5 mm by setting the flange height to 14 mm, which is twice the flange height in the case of compressor for air conditioner.

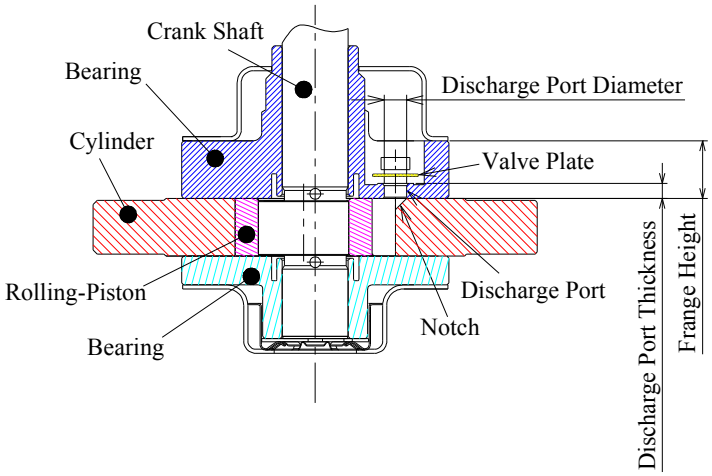

Figure 6: Cross section of compression Mechanism

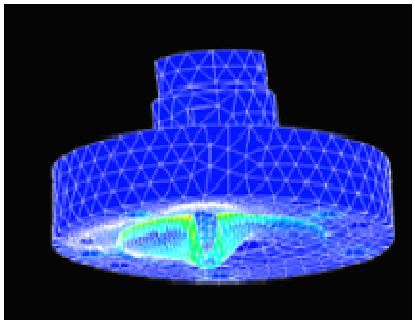

Figure 7: Example of deformation analysis result

Table 2: Result of deformation analysis by FEM

Frange Height	[mm]	7.0		14.0	
Discharge Port Thickness	[mm]	3.7	2.5	3.7	2.5
result	[-]	○	×	◎	○
deformation ratio	[%]	100%	137%	58%	100%

◎: Exellent ○: good ×: NG

Figure 8 shows the results of investigating the relationship between COP and operation speed with different discharge-port diameters in the case in which the notch in the cylinder was eliminated, the position of the discharge port was changed, and the height of the discharge port was set to be 2.5 mm. Between the discharge-port diameters of 5.0 and 4.5 mm, the COP for the diameter of 4.5 is higher on the low-speed side and, in contrast, is lower on the high-speed side. In addition, when the port diameter is reduced to 4.0 mm, where the area of the port corresponds to 64 % of the area at the diameter of 5.0 mm, the COP deteriorated at all operation speeds. The COPs at diameters of 4.5 mm and 5.0 mm were equivalent at $50s^{-1}$, that is, the intermediate capacity range. The diameter of 5.0 mm was selected because the volumetric efficiency is higher at high operation speed, and this is advantageous in ensuring that the maximum capacity is achieved.

As shown in Figure 9, by re-examining the discharge port and the notch in the cylinder in this study, we succeeded in reducing the dead volume to half the original volume.

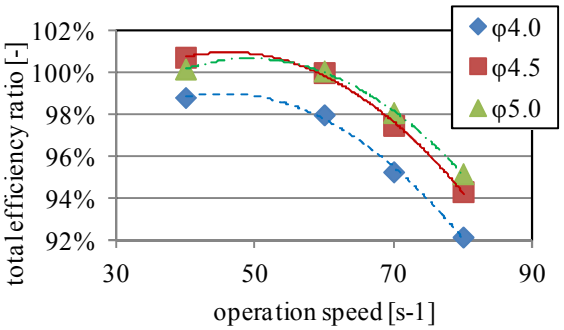

Figure 8: Relationship between operational speed and total efficiency ratio

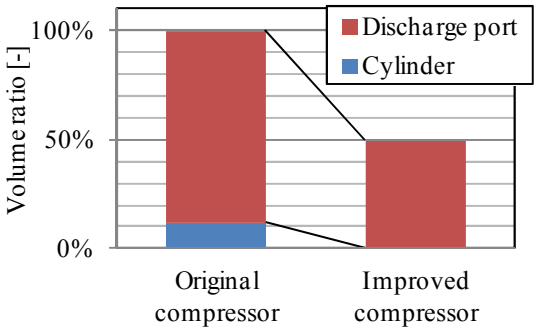

Figure 9: Comparison of dead volume ratio

3.2 Improved motor

Although the motor specifications of the original compressor were designed for achieving good efficiency in a wide operating range, in this study, focusing on the intermediate capacity range, we re-examined the number of windings and the total height of the motor core and successfully increased the flux level of the motor by a factor of 1.2. Figure 10 shows the relationship between the rotational speed and the motor efficiency. At $50s^{-1}$, which is the intermediate capacity range that contributes to the APF, we achieved a 2 % improvement in efficiency. Figure 11 shows the relationship between the rotational speed and COP for the original and improved compressors. With the improved compressor, we were able to improve the COP in the range centered around the intermediate capacity range, as compared with the original compressor.

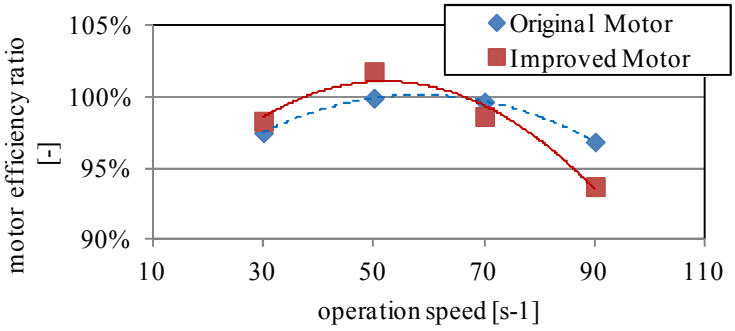

Figure 10: Relationship between operation speed and motor efficiency ratio

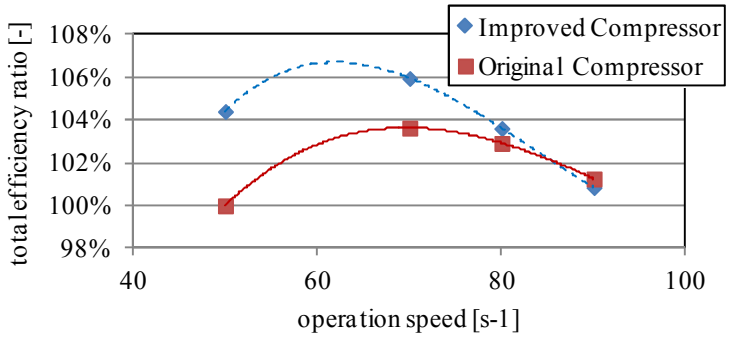

Figure 11: Relationship between operation speed and total efficiency ratio

4. NOISE REDUCTION

4.1 Problems to be addressed

Figure 12 shows the results of analyzing noise from the original compressor when accelerating from $45s^{-1}$ to $100s^{-1}$. In this figure, the horizontal axis indicates noise frequency and the vertical axis indicates time. Sound pressure is indicated by different colors, where red is the highest, followed by green and blue, and sound pressures below these are indicated by white. From this figure, it is clear that there are portions with high sound-pressure levels centered around 1200 Hz, irrespective of the rotational speed. As described above, this frequency band corresponds to a region in which it is difficult to achieve sound insulation using a soundproofing material and a housing. In this study, we investigated noise reduction in this 1.25-kHz band.

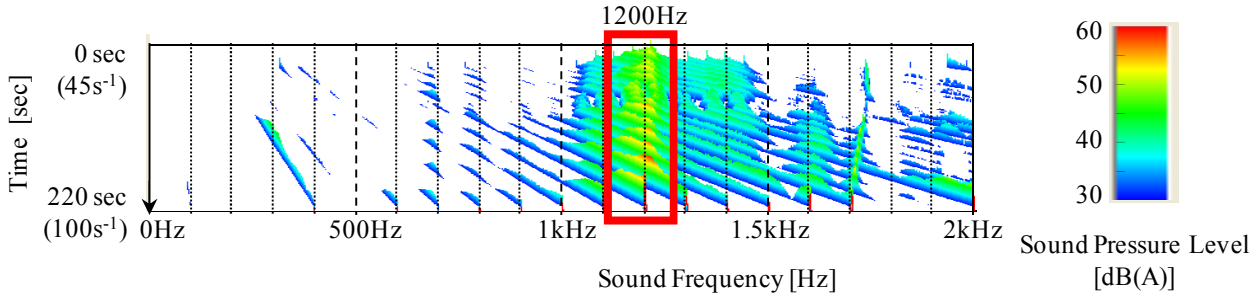

Figure 12: The result of run-up test (from $45s^{-1}$ to $100s^{-1}$)
(Measurement point: 1 m from bottom center of main body. Direction: Accumulator, Height: 0.45 m)

4.2 Method for Analyzing

4.2.1 Modal Analysis: We created an FEM model of the entire compressor and performed a modal analysis. Figure 13 shows the model used for the analysis and the result of analyzing the mode shape at 1284 Hz. This figure shows a mode in which the bottom portion of the accumulator vibrates in the radial direction with respect to the compressor main unit.

4.2.2 Radiation Surface Analysis by a Sound particle velocity probe: Radiation surface analysis was performed in order to check whether or not sound is radiated from a surface in the radial direction at the bottom portion of the accumulator during the actual operation. In general, sound pressure has no directionality and a high sound pressure is recorded when there is a source of loud sound in the vicinity, whereas both acoustic particle velocity and sound intensity have directionality and exhibit greater sensitivity for sound coming from the surface at which a sensor is pointed. Therefore, it is possible to identify the actual radiation surface with greater precision by using acoustic particle velocity map or sound intensity map. However, with a sound intensity probe with a paired microphone system, like that shown in Figure 15 (a), it has been difficult to take measurements at an intermediate portion between the accumulator and the compressor main unit, restricted by the size of the probe itself. Figure15 (b) shows acoustic particle velocity probes that have become commercially available in recent years. The size of acoustic particle velocity probes is about the same size as a 1/2-inch microphone, and a sensor that can directly measure acoustic particle velocity and a microphone are provided side-by-side at the tip, making it possible to measure sound pressure, acoustic particle velocity, and sound intensity at the same time. Figure 14 shows a sound-intensity map created by using such an acoustic particle velocity probe. The sound-intensity levels were high at the bottom portion of the accumulator specifically. This result agrees well with the result of modal analysis. Thus, we considered a resonance that vibrates in the radial directions at the bottom portion of the accumulator to be the cause of increased noise in the 1.25-kHz band.

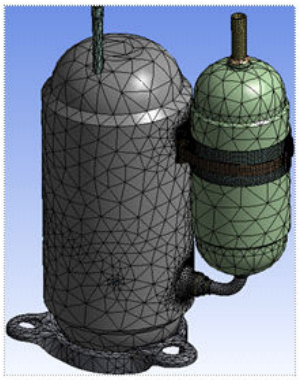

Model

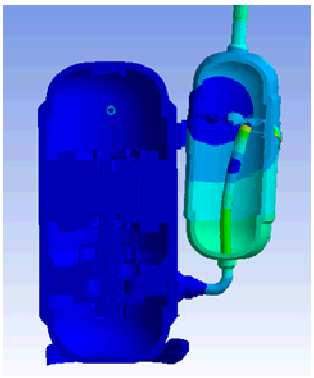

Result (1284Hz)

Figure 13: Modal analysis by FEM

1.25-kHz band

Figure 14: Sound Intensity Map of Original Compressor

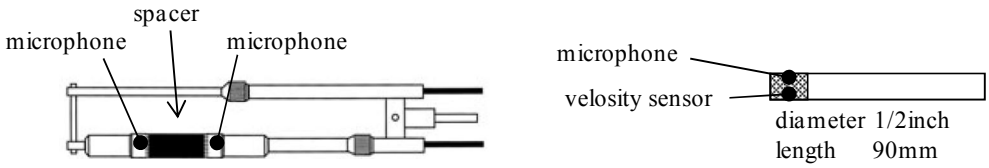

(a) typical intensity probe

(b) acoustic particle velocity probe

Figure 15: Comparison of acoustic-particle-velocity probe and typical sound-intensity probe.

4.3 Noise Reduction Measure

In this study, we investigated whether or not it is possible to reduce noise in the 1.25-kHz band by shifting the resonance frequency of the accumulator toward the high-frequency side by changing the diameter and height of the accumulator, without changing the volume for liquid refrigerant to be accumulated, in consideration of past performance in achieving reliability.

Figure 17 shows a sound intensity map of a compressor employing an accumulator with a small diameter shown in Figure 16. As compared with the map shown in Figure 14, it was confirmed that sound radiated from the accumulator was considerably reduced. Subsequently, we checked a noise map for the 1.6-kHz band in order to confirm that the frequency at which the bottom portion of the accumulator resonates shifted toward the high-frequency side. Figure 18 displays noise maps, respectively showing sound pressure, acoustic particle velocity, and sound intensity. There was high radiation from the bottom portion of the accumulator, and it was confirmed that the above-described characteristic value of the accumulator shifted from the 1.25-kHz band to the 1.6-kHz band. In addition, it was also confirmed that the radiation surfaces were distinguished with greater precision in the intensity map and the acoustic particle velocity map, as compared with the sound-pressure map. Finally, Figure 19 shows the results of sound power level measurements as compared with the original compressor. By making changes in the accumulator, 1.6-kHz band got worse, but the 1.25-kHz was highly improved. We were able to improve the noise of compressor.

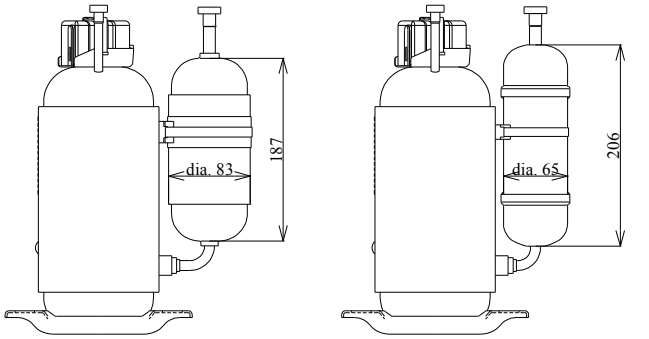

Compressor with Original Accumulator

Compressor with Improved Accumulator

Figure 16: The exterior view of compressors

1.25-kHz band

Figure 17: Sound intensity map of improved compressor

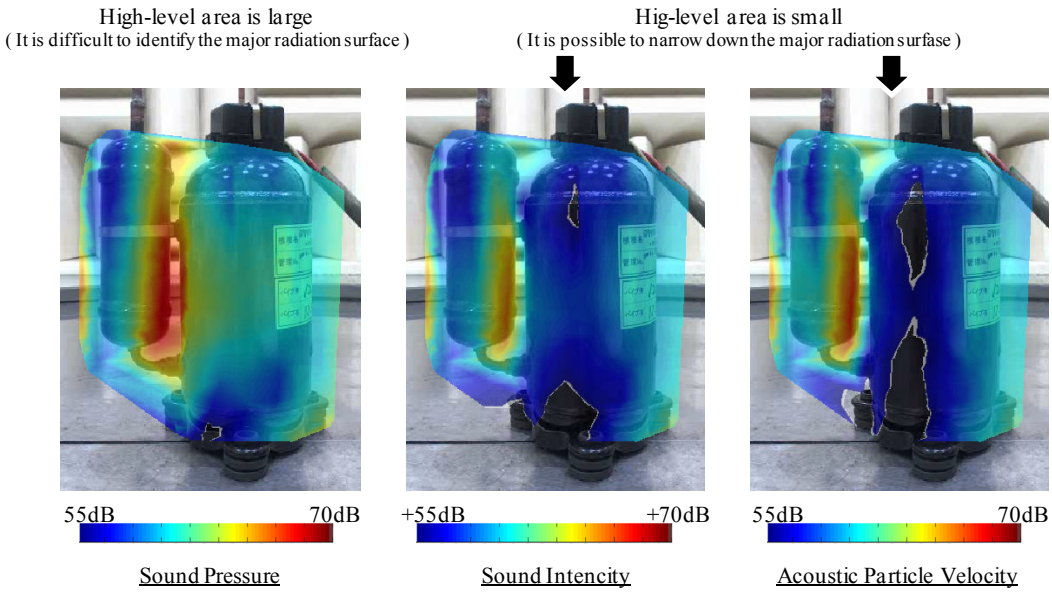

Figure 18: Sound maps of improved compressor, 1.6-kHz band

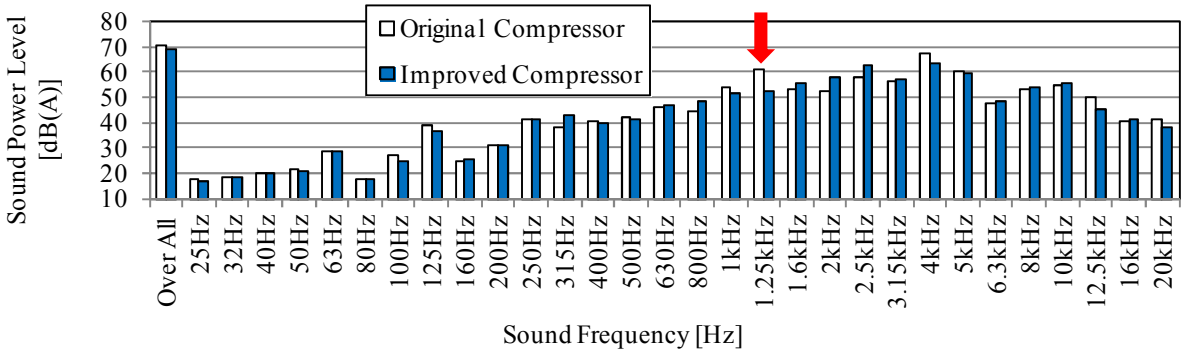

Figure 19: Comparison of sound power level

6. CONCLUSIONS

We have developed a high-APF, low-noise CO2 rotary compressor.

- We found that, for a CO2 rotary compressor also, optimizing the design of the discharge pathway from the compression chamber, including the discharge-port diameter, and adjusting the flux level of the motor are effective for enhancing the COP in the intermediate capacity range.
- We confirmed that, to develop measures against noise due to a transfer system such as an accumulator or the like, it is effective to employ modal analysis based on FEM and radiation surface analysis using an acoustic particle velocity probe, which can measure the intensity and particle velocity even in a small space.

REFERENCES

Agency for Natural Resources and Energy, 2013, *FY2013 Annual Energy Report*, Shin-kosoku-insatsu, Niigata: p.108

Koyama, S., Ito, D., Lee, S., Kuwahara, K., Saeki, C., 2005, Experimental Study on Flow Boiling of CO2-PAG Oil Mixture in Smooth and Micro-fin Tubes, *Trans. of the JSRAE*, vol. 22, no. 4: p. 385-393